Front. Optoelectron. China 2011, 4(4): 430–433
DOI 10.1007/s12200-011-0173-6

RESEARCH ARTICLE

Axial strain sensitivity analysis of long period fiber grating by new transfer matrix method

Guodong WANG (✉), Yunjian WANG, Na LI

School of Electrical Engineering and Automation, Henan Polytechnic University, Jiaozuo 454003, China

© Higher Education Press and Springer-Verlag Berlin Heidelberg 2011

Abstract The axial strain sensitivity of long period fiber grating (LPFG) is analyzed by new transfer matrix method. The new transfer matrix method can be used to analyze the modes coupling between the core mode and multiple cladding modes. Compared with the previous method used, such as solving the coupled mode equation by the fourth order adaptive step size Runge-Kutta algorithm, the new transfer matrix method (TMM) has a faster calculation speed. Theoretical results are excellent agreement with the method of solving the coupled mode equation (SCME).

Keywords axial strain sensitivity, long period fiber grating (LPFG), new transfer matrix method (TMM)

1 Introduction

Long period fiber gratings (LPFGs) have been found many applications in optical telecommunications such as mode converters [1], rejection filters [2], gain-flattening filters for erbium-doped fiber amplifiers [3], optical fiber sensors for strain [4], temperature [5], and refractive index measurements [6] because of their capability to couple power between core and cladding modes at resonant wavelengths [7–10].

The strain sensitivity of LPFG can be obtained by analyzing spectral variation under different strain. The common methods used to analyze the spectral characteristics of LPFG and fiber Bragg gratings include transfer matrix method (TMM) and solving the coupled mode equations (SCMEs) [11–13]. The traditional TMM is able to analyze the uniform and non-uniform LPFG and fiber Bragg gratings when only two modes are considered [14,15]. The SCME method can obtain the spectrum of the uniform and non-uniform structure LPFG when multiple modes are considered. In this paper, a new TMM about LPFG with multiple cladding modes coupled is proposed and applied to analyze the axial strain sensitivity of LPFG. This new TMM can be used to analyze the modes coupled both about the uniform and the non-uniform between the core mode and the multiple cladding modes. And the new TMM is simple to implement, almost always sufficiently accurate, and generally faster than that of SCME.

Received June 8, 2011; accepted June 28, 2011

E-mail: wgd@hpu.edu.cn

2 New transmission matrix

The coupled-mode equations of LPFG are given as [14]

$$\begin{cases} \dfrac{\mathrm{d}A^{\mathrm{co}}}{\mathrm{d}z} = \mathrm{j}k_{01-01}^{\text{co-co}}A^{\mathrm{co}} + \mathrm{j}\sum\limits_{v}\dfrac{m}{2}k_{1v-01}^{\text{cl-co}}A_v^{\mathrm{cl}}\mathrm{e}^{-\mathrm{j}2\delta_{1v-01}^{\text{cl-co}}z}, \\ \sum\limits_{v}\left[\dfrac{\mathrm{d}A_v^{\mathrm{cl}}}{\mathrm{d}z} = \mathrm{j}\dfrac{m}{2}k_{1v-01}^{\text{cl-co}}A^{\mathrm{co}}\mathrm{e}^{\mathrm{j}2\delta_{1v-01}^{\text{cl-co}}z}\right], \end{cases} \tag{1}$$

where A^{co} is the amplitude for the core mode, A^{cl} is the amplitude for the cladding mode HE_{1v}, $k_{01-01}^{\text{co-co}}$ is the coupling constant for core-mode –core-mode, $k_{1v-01}^{\text{cl-co}}$ is the coupling constant for core-mode –cladding-mode.

$$\delta_{1v-01}^{\text{cl-co}} = \frac{1}{2}\left(\beta_{01}^{\mathrm{co}} - \beta_{1v}^{\mathrm{cl}} - \frac{2\pi}{\Lambda}\right), \tag{2}$$

where β_{01}^{co} and β_{1v}^{cl} are the propagation constant of the core mode and cladding mode, and Λ is the period of grating.

If defined S_v as

$$S_v = A_v^{\mathrm{cl}}\mathrm{e}^{-\mathrm{j}2\delta_{1v-01}^{\text{cl-co}}z}, \tag{3}$$

follow equations can be obtained as

$$\begin{cases} \dfrac{\mathrm{d}A^{\mathrm{co}}}{\mathrm{d}z} = \mathrm{j}k_{01-01}^{\text{co-co}}A^{\mathrm{co}} + \sum\limits_{v}\mathrm{j}\dfrac{m}{2}k_{1v-01}^{\text{cl-co}}S_v, \\ \sum\limits_{v}\left[\dfrac{\mathrm{d}S_v}{\mathrm{d}z} = \mathrm{j}\dfrac{m}{2}k_{1v-01}^{\text{cl-co}}A^{\mathrm{co}} - \mathrm{j}2\delta_{1v-01}^{\text{cl-co}}S_v\right]. \end{cases} \tag{4}$$

Then, the matrix form of Eq. (4) can be expressed as

$$\begin{bmatrix} \frac{dA^{co}}{dz} \\ \frac{dS_1}{dz} \\ \vdots \\ \frac{dS_v}{dz} \end{bmatrix} = \boldsymbol{F} \begin{bmatrix} A^{co} \\ S_1 \\ \vdots \\ S_v \end{bmatrix}. \tag{5}$$

If defined a vector $\boldsymbol{A}$ as

$$\boldsymbol{A} = \begin{bmatrix} A^{co} \\ S_1 \\ \vdots \\ S_v \end{bmatrix}, \tag{6}$$

Eq. (4) can be expressed as

$$\frac{d\boldsymbol{A}}{dz} = \boldsymbol{FA}, \tag{7}$$

where

$$\boldsymbol{F} = j \begin{bmatrix} k^{\text{co-co}}_{0,1-01} & \frac{m}{2}k^{\text{cl-co}}_{1,1-01} & \frac{m}{2}k^{\text{cl-co}}_{1,2-01} & \cdots & \frac{m}{2}k^{\text{cl-co}}_{1,v-1-01} & \frac{m}{2}k^{\text{cl-co}}_{1,v-01} \\ \frac{m}{2}k^{\text{cl-co}}_{1,1-01} & -2\delta^{\text{cl-co}}_{1,1-01} & 0 & \cdots & 0 & 0 \\ \frac{m}{2}k^{\text{cl-co}}_{1,2-01} & 0 & -2\delta^{\text{cl-co}}_{1,2-01} & 0 & \cdots & 0 \\ \vdots & \vdots & 0 & \ddots & 0 & \vdots \\ \frac{m}{2}k^{\text{cl-co}}_{1,v-1-01} & 0 & \vdots & 0 & -2\delta^{\text{cl-co}}_{1,v-1-01} & 0 \\ \frac{m}{2}k^{\text{cl-co}}_{1,v-01} & 0 & 0 & \cdots & 0 & -2\delta^{\text{cl-co}}_{1,v-01} \end{bmatrix}. \tag{8}$$

For the uniform grating, $\boldsymbol{F}$ is a constant, Eq. (7) is a linear constant coefficient difference equation. The form of the solution of Eq. (7) can be expressed as

$$\boldsymbol{A}(z) = \boldsymbol{A}_0 e^{\boldsymbol{F}z}, \tag{9}$$

where $\boldsymbol{A}_0$ is the initial value of the vector at $z = 0$ position, and can be expressed as

$$\boldsymbol{A}_0 = [1,0,\cdots 0]'. \tag{10}$$

So, the transfer matrix of the uniform LPFG can be expressed as

$$\boldsymbol{T} = e^{\boldsymbol{F}L}, \tag{11}$$

where L is the grating length.

So the transmission rate of core mode can be expressed as

$$\rho = \frac{A^{co}(L)}{A^{co}(0)} = A^{co}(L). \tag{12}$$

For the non-uniform LPFG the grating can be divided into hundreds segments, and every segment can be considered as uniform. The transfer matrix of the ith segment can be expressed as

$$\boldsymbol{T}_i = e^{\boldsymbol{F}L_i}, \tag{13}$$

where L_i is the length of ith segment. The total transfer matrix of the grating can be expressed as

$$\boldsymbol{T} = \boldsymbol{T}_0 \boldsymbol{T}_1 \cdots \boldsymbol{T}_N. \tag{14}$$

3 Axial strain sensitivity analysis

In this section, we analyze the axial strain sensitivity of LPFG by the new TMM as described above. The fiber considered in this paper is of a step-index profile and a three layers structure. The parameters of the fiber are given as: the core radius $r_1 = 2.625$ μm, the cladding radius $r_2 = 62.5$ μm, the core index $n_1 = 1.458$, the cladding index $n_2 = 1.45$ and the air index $n_3 = 1.0$.

Firstly, in order to prove the correctness of the new TMM, a Blackman apodization LPFG is analyzed. The transmission spectrum of this grating is shown in Fig. 1 (solid line). The grating parameters are given as: grating period $\Lambda = 470$ μm, grating length $L = 25$ mm, the peak induced-index change is 0.0001. The five main dips shown in the spectrum are the result from the coupling between the core mode and the v = 1, 3, 5, 7, 9 cladding modes. For comparison, the transmission spectrum of this grating is calculated again by the SCME, which is illustrated in Fig. 1 (dotted line). From Fig. 1 it can be obtained that the new TMM is exactly enough to analyze the transmission spectrum of LPFG.

Compared with the SCME method, the advantage of the new TMM is that it can analyze the transmission characteristic of non-uniform LPFG with a faster speed. In order to compare the calculating speed of these two methods, the computing time is illustrated in Fig. 2 when different cladding modes have been considered. It can be found that the calculating speed by the new TMM is faster than that by SCME.

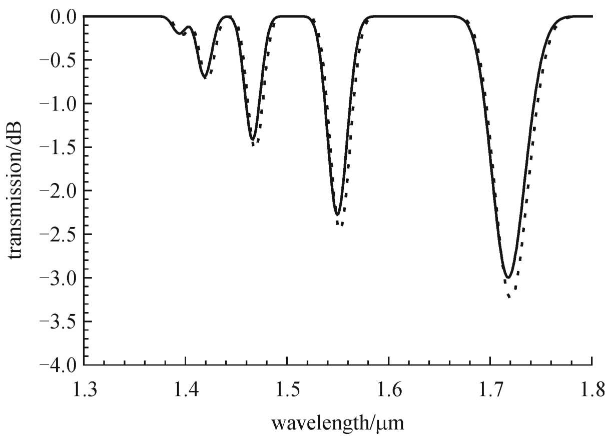

Fig. 1 Theoretically calculated transmission spectrum by new TMM (solid line) and SCME (dotted line) through a Blackman apodization grating

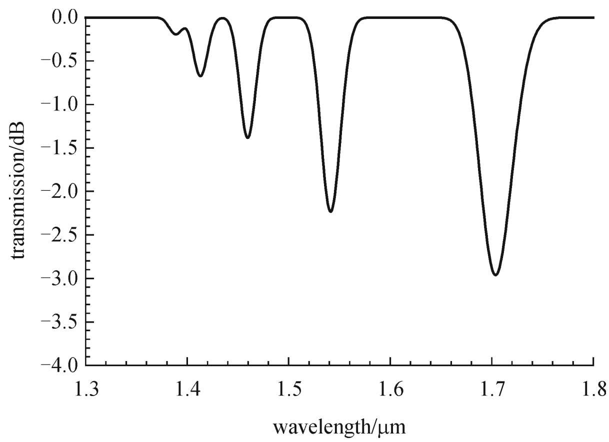

Fig. 3 Theoretically calculated transmission spectrum by new TMM through a non-uniform period grating

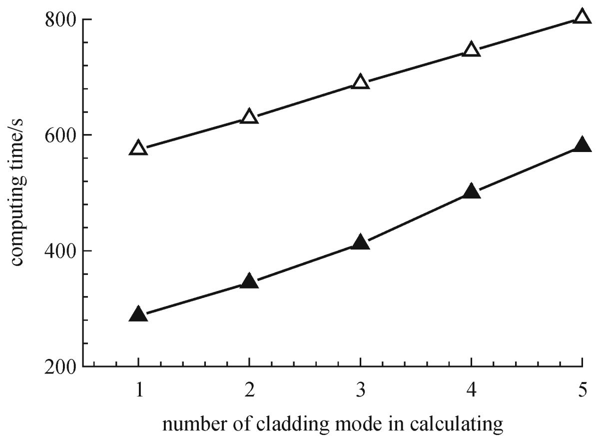

Fig. 2 Computing times for new TMM (▲) and SCME (△)

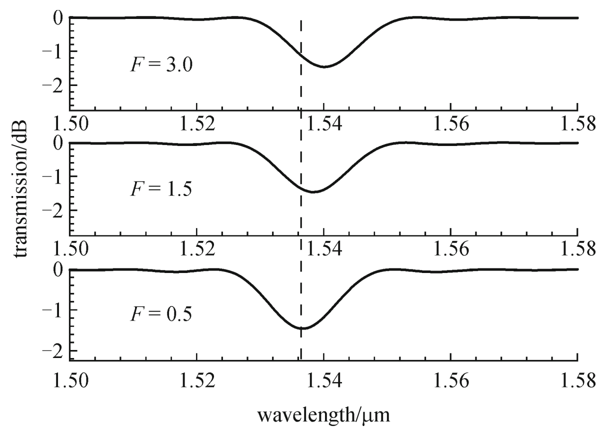

Fig. 4 Transmission spectral of LPFG when different tension F is applied to it

The new TMM can be also used to analyze the transmission characteristic of non-uniform LPFG. The theoretical calculated through a non-uniform period LPFG is indicated in Fig. 3.

When the grating is held under the tension, an axial strain $\varepsilon(z)$ will be produced along the grating length, which can be given by

$$\varepsilon(z) = \frac{\boldsymbol{F}}{E\boldsymbol{A}(z)}, \tag{15}$$

where $\boldsymbol{A}(z)$ is the cross-section area of grating at position z, E is Young's modulus of fiber. Because of the existence of E, the period of the grating and the effective index of transmission modes in fiber will be changed along the grating length, and can be expressed as

$$\Lambda(z) = \Lambda_0[1 + \varepsilon(z)], \tag{16}$$

$$n(z) = n_{\text{eff}} - \chi\varepsilon(z), \tag{17}$$

where Λ_0 is the grating period at position $z = 0$, $\Lambda(z)$ is the grating period at position z, χ is the elasto-optical coefficient of fiber and n_{eff} is the effective index of transmission mode in fiber.

Figure 4 shows the transmission spectrum of LPFG when different tension F is applied to the grating. The resonance shown in Fig. 4 is associated with coupling between the core mode and the $v = 7$ cladding mode. The coupled wavelength will shift to the longer wavelength when a certain tension is applied to the grating. The more details on the wavelength shift about more cladding mode are demonstrated in Fig. 5. From these figures we can find that the larger the tension applied to the grating, the farther wavelength shifts.

4 Conclusions

In this paper, a new transfer matrix method about long

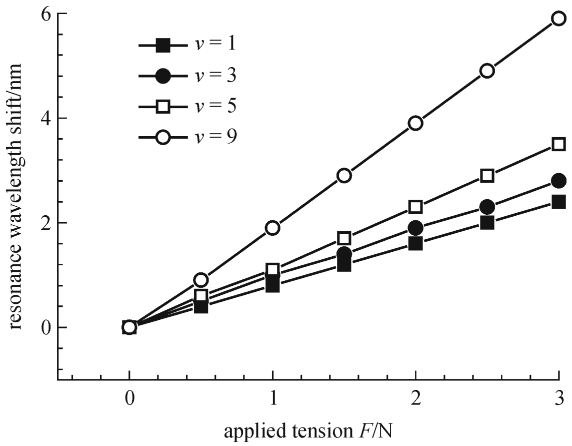

Fig. 5 Resonance wavelength of LPFG when different tension F is applied to it

period fiber grating with multiple cladding modes is proposed. The new method can be used to analyze the axial strain sensitivity of long period fiber grating. Compared with the usually used method, such as solving the coupled mode equation by the fourth order adaptive step size Runge-Kutta algorithm, the new transfer matrix method is of a faster calculation speed. The theoretical results are exactly agreed with the method of solving the coupled mode equation.

Acknowledgements This work was supported by the National Natural Science Foundation of China (Grant No. 61040016), the Open Foundation from Henan Provincial Open laboratory of Control Engineering Key Disciplines China (No. KG2009-16) and the Doctor Foundation from Henan Polytechnic University China (No. 648393).

References

1. Andermahr N, Fallnich C. Optically induced long-period fiber gratings for guided mode conversion in few-mode fibers. Optics Express, 2010, 18(5): 4411–4416
2. Chen K, Sheng Q Q, Dong X Y. Band-rejection and band pass filters based on mechanically induced long-period fibergratings. Microwave and Optical Technology Letters, 2004, 42(1): 15–17
3. Ni N, Chan C C, Tan K M, Tjin S C, Dong X Y. Broad-band EDFA gain flattening by using an embedded long-period fiber grating filter. Optics Communications, 2007, 271(2): 377–381
4. Kang J, Dong X Y, Zhao C L, Qian W W, Li M C. Simultaneous measurement of strain and temperature with a long period fiber grating inscribed Sagnac interferometer. Optics Communications, 2011, 284(8): 2145–2148
5. Venugopalan T, Sun T, Grattan K T V. Temperature characterization of long period gratings written in three different types of optical fiber for potential high temperature measurements. Sensors and Actuators A, Physical, 2010, 160(1–2): 29–34
6. Martinez-Rios A, Monzon-Hernandez D, Torres-Gomez I. Highly sensitive cladding-etched arc-induced long period fiber gratings for refractive index sensing. Optics Communications, 2010, 283(6): 958–962
7. Harhira A, Guay F, Daigle M, Lapointe J, Kashyap R. Long-period fiber gratings fabricated with a CO_2 laser beam and phase mask. Optics Communications, 2010, 283(23): 4633–4638
8. Eggen C L, Lin Y S, Wei T, Xiao H. Detection of lipid bilayer membranes formed on silica by double-long period fiber grating laser refractometry. Sensors and Actuators B, Chemical, 2010, 150 (2): 734–741
9. Nam S H, Lee J, Yin S Z. Control of resonant peak depths of tunable long-period fiber gratings using over coupling. Optics Communications, 2011, 284(4): 961–964
10. Jiang M S, Feng D J, Sui Q M. Characteristic research on mechanically induced long-period fiber gratings. Chinese Optics Letters, 2009, 7(2): 112–114
11. Wang G D, Xie B B. Improving the performance of chirped fiber grating with cladding being etched sinusoidal function. Optik (Stuttgart), 2011, 122(6): 557–559
12. Dong X W, Feng S C, Xu O, Lu S H, Pei L. Add/drop channel filter based on two parallel long-period fiber gratings coupler. Optik (Stuttgart), 2009, 120(16): 855–859
13. Shao L Y, Laronche A, Smietana M, Mikulic P, Bock W J, Albert J. Highly sensitive bend sensor with hybrid long period and tilted fiber Bragg grating. Optics Communications, 2010, 283(13): 2690–2694
14. Erdogan T. Cladding-mode resonances in short- and long-period fiber grating filters. Journal of the Optical Society of America A, 1997, 14(8): 1760–1773
15. Erdogan T. Fiber grating spectra. Journal of Lightwave Technology, 1997, 15(8): 1277–1294